

PAPER

Effect of surface topography and roughness on the leakage of static seals

To cite this article: Zhengpeng Gu *et al* 2024 *Surf. Topogr.: Metrol. Prop.* **12** 025014

View the [article online](#) for updates and enhancements.

You may also like

- [Metal rough surface leakage model based on porous percolation theory](#)
Ying Lin, Wanqin Zhu, Xinhai Yu et al.
- [Simulation analysis of metal gasket's sealing performance in High-pressure pipe of launch vehicle](#)
Peng Yu, Zechen Li, Jinlong Yu et al.
- [Hybrid and electric vehicle tribology: a review](#)
Hemanth G, Suresha B and Ananthapadmanabha

Surface Topography: Metrology and Properties



PAPER

Effect of surface topography and roughness on the leakage of static seals

RECEIVED
9 January 2024

ACCEPTED FOR PUBLICATION
30 April 2024

PUBLISHED
9 May 2024

Zhengpeng Gu, Qingwen Dai , Wei Huang and Xiaolei Wang

College of Mechanical and Electrical Engineering, Nanjing University of Aeronautics and Astronautics, Nanjing, 210016, People's Republic of China

E-mail: daiqingwen@nuaa.edu.cn

Keywords: static seals, leakage, surface topography, roughness, grinding scars

Supplementary material for this article is available [online](#)

Abstract

Static seal is widely used in modern machinery. Leakage of static seals would shorten the mechanical system's service life and affect the environment. To understand the leakage characteristics of static seals, in this work, an experimental apparatus for leakage quantization was built. The effects of surface topography and roughness on the leakage performance of static seals subject to elevated pressure were highlighted. It was found that the leakage rate is negatively correlated with contact pressure. Orientation of surface topography affects the leakage, where the grinding scar parallel to the leakage direction contributes to the leakage, and the perpendicular grinding scar has an inhibiting effect. The leakage rate of irregular and discontinuous surface topography is lower than that of regular ones, and it increases with increasing surface roughness. Furthermore, the leakage mechanism of surface topography and roughness was revealed. This work provides general guidance for the parameters design of static seals.

1. Introduction

Sealing technology is of great significance to the reliable operation of mechanical equipment, resource conservation, and environmental protection [1]. Sealing structures are divided into static and dynamic seals based on the relative motion of sealing interfaces [2]. Static seal refers to the sealing between two contact surfaces stabilized by a specific preload [3]. It has obvious advantages of low leakage, elimination of contact friction, and low power consumption, which is widely used in many applications, including petrochemical engineering [4], deep-sea construction [5], aerospace exploration [6], etc.

Static seals' sealing performance is directly related to the quality of the two contact surfaces. To understand the effect of surface quality on sealing performances, Arghavani [7] *et al* investigated the leakage rate of static seals with various surface topographies obtained by grinding, turning, and milling processing methods, respectively. At low-stress levels, the rougher ground and milled sealing surfaces with radial channels produce larger leakage rates. Zhang *et al* [3] measured the leakage rate of static seals with surfaces of

isotropic and anisotropic microstructures and established a simplified leakage prediction model with high accuracy. Goltsberg *et al* [8] found that for static seals made of polymer materials, the sealing performance was in positive correlation with the contact pressure and negative correlation with surface roughness. Marie *et al* [9] studied the fluid leakage between sapphire and metal interfaces and found that it reproduces linear dependence of the flow rate on the driving force.

Theoretical investigations on static seals mainly focus on contact modeling, which is established via Hertz contact theory [10], statistical G-W contact model [11], fractal theory based M-B contact model [12], or two-dimensional percolation grid model [13–17]. In these models, the sealing interface is simplified to a contact surface between a rigid plane and a rough surface, and the height characteristics of the surfaces are ignored [18, 19]. These models lay the groundwork for subsequent contact modeling improvements and predicting leakage.

To improve the sealing performance of static seals and explore the sealing mechanism, researchers have carried out abundant investigations on the sealing

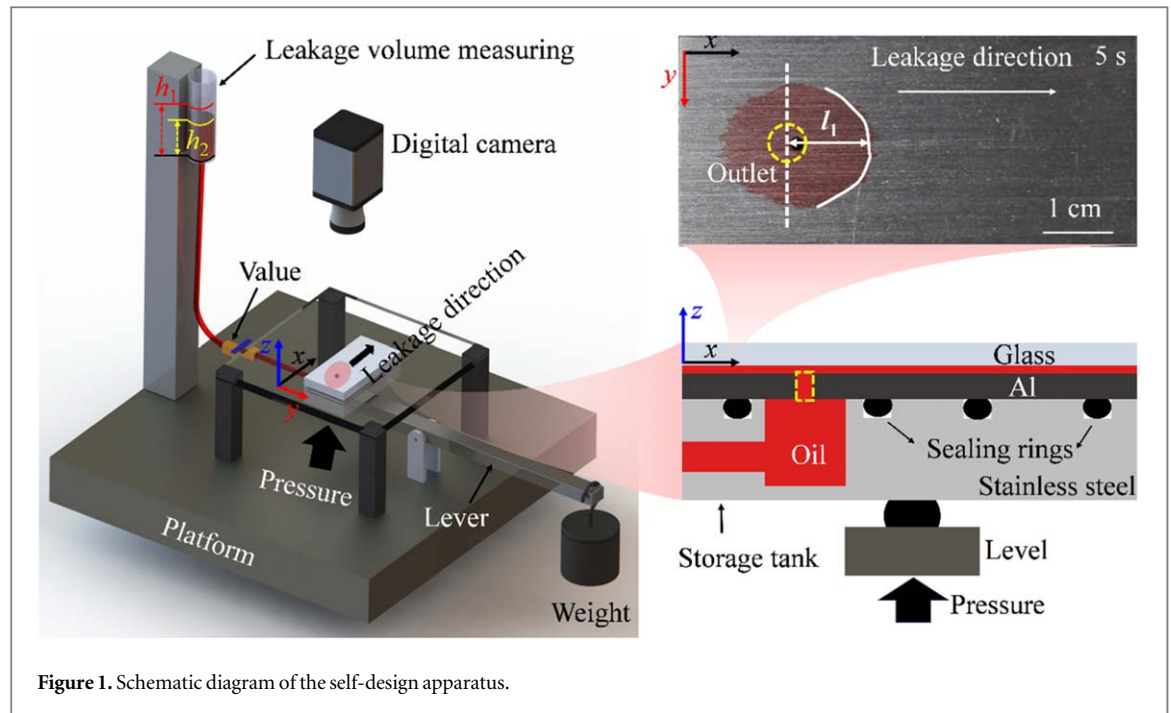


Figure 1. Schematic diagram of the self-design apparatus.

performance of static seals from experimental and theoretical aspects, which provides valid references for improving the performances of static seals, as well as the understanding of the static sealing mechanism. Note that all engineering surfaces are rough and with macro-, micro-, or nano-scaled structures. When two surfaces are in direct contact, the peaks and troughs of the rough surface are interlaced to form pores of different sizes. Once the contact pressure is changed, the pores will be connected to form one or several leakage channels, affecting the seal performance [3, 19].

Nowadays, with the development of modern industry, the emergence of various extreme service conditions has raised the bar for the design of static seals. Different machining processes generate varying surface topographies and roughness, for these real machining surfaces: it is unknown how the influence law evolves under different contact pressures or other complex sealing conditions, and for static seals with different surface topography under real working conditions, it is difficult to accurately predict the leakage rate of via the above-mentioned contact models, since simplified contact models yield a deviation of the prediction. A comprehensive and systematic investigation on the effects of surface morphology and surface roughness on sealing performance at different contact pressures is essential.

Hence, in this work, the sealing performances of static seals were investigated. An experimental apparatus for observing leakage rate was constructed, and specimens with different grinding scar directions and roughness were prepared. The effects of contact pressure, surface topography, and roughness were investigated, and the leakage mechanism of different surface topography and roughness were revealed. The

findings proposed in this work provide a reference for the design of a static sealing face.

2. Material and methods

2.1. Apparatus and test procedure

Figure 1 shows the schematic diagram of the apparatus designed in this study. An oil storage tank made of stainless steel with a dimension of 60 mm × 30 mm × 15 mm was connected to a pipe for oil supply from the measuring cylinder. A glass plate (SiO₂, 60 mm × 30 mm × 2 mm) and an aluminum alloy plate (Al, 60 mm × 30 mm × 3 mm) were mounted right above the oil storage tank. On the top, a plexiglass plate (Polymethyl methacrylate, PMMA, 100 mm × 100 mm × 10 mm) was used to hold down the glass, and a lever was fixed right below the oil storage tank, with a specific dead weight, a controllable contact pressure could be created between the interface. The whole apparatus was fixed to a platform. No.10 aviation hydraulic oil was adopted for the leakage experiments, and it could flow into the interface of glass and Al plates via the through-hole in the Al plate. All experimental conditions are shown in table 1.

The experimental process is as follows: opening the value to allow the oil to flow into the interface, the oil firstly spreads around from the middle hole, and after reaching the boundary (y-direction), the oil leaks in the x-direction direction, and the digital camera captures the leakage process. Keyframes are extracted from the video, and the oil leakage velocity (equation (1)) is calculated by the image and video editing software. The leakage rate (equation (2)) was calculated by measuring the drop height difference of

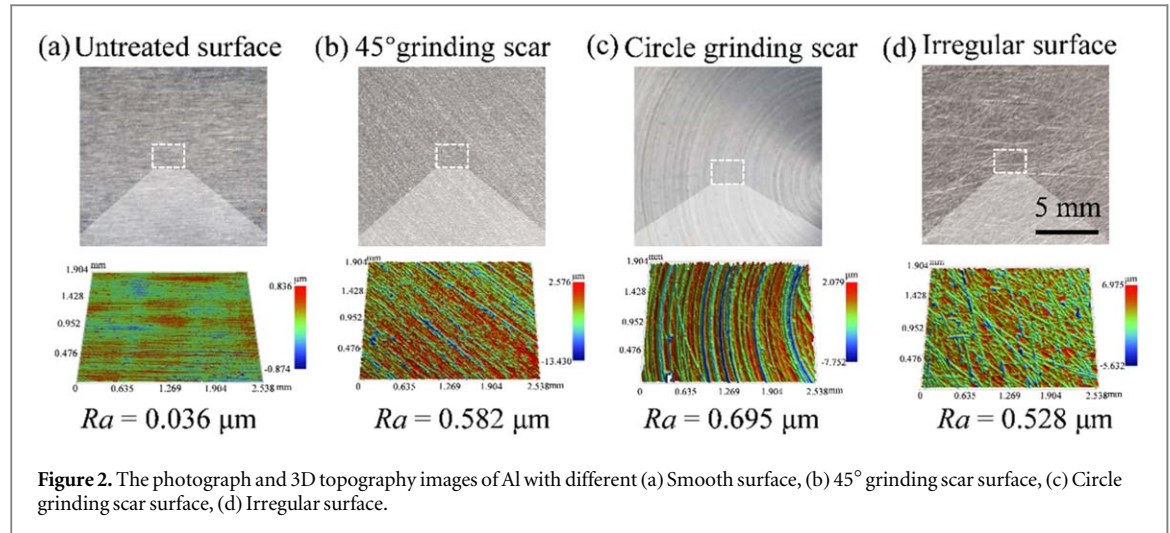


Figure 2. The photograph and 3D topography images of Al with different (a) Smooth surface, (b) 45° grinding scar surface, (c) Circle grinding scar surface, (d) Irregular surface.

Table 1. Experimental conditions.

Parameter	Value
Environment temperature	25 °C
Experimental liquid	No.10 aviation hydraulic oil
Kinematic viscosity	10 mm ² /s
Density	850 kg m ⁻³
Surface tension	33.7 mN/m
Contact pressure	0.01–0.07 MPa

the interface inside the measuring cylinder per time.

$$V = \frac{l_1}{t} \quad (1)$$

$$Q = \frac{\pi r^2 (h_1 - h_2)}{t} \quad (2)$$

Although under practical engineering applications, the range of contact pressure is about 0.5 ~ 110 MPa, and the internal oil pressure is also very high (0 ~ 42 MPa). In this work, equivalent experiments with a low contact pressure and low oil pressure were carried out to understand the effect of surface topography and roughness on the leakage of static seals.

2.2. Specimen preparation and characterization

In this study, the untreated glass has a low surface roughness of 0.02 μm, so we termed it as smooth. In addition, the Al and glass surfaces with different roughness and grinding scars were fabricated. The detailed processing is as follows: the Al and glass surfaces were polished with different particle sizes (200#, 400#, 800#, 1000#, 1400#) to obtain test surfaces with different roughness. Surfaces with parallel, 30, 45, 60, and perpendicular grinding scars were obtained by means of reciprocal grinding, circle grinding scars by means of rotation, and irregular grinding scars by means of non-directional grinding. Processing parameters and conditions were consistent across all test surfaces during the grinding process.

Figure 2 shows the surface topography, roughness, and geometric dimensions of four typical prepared Al

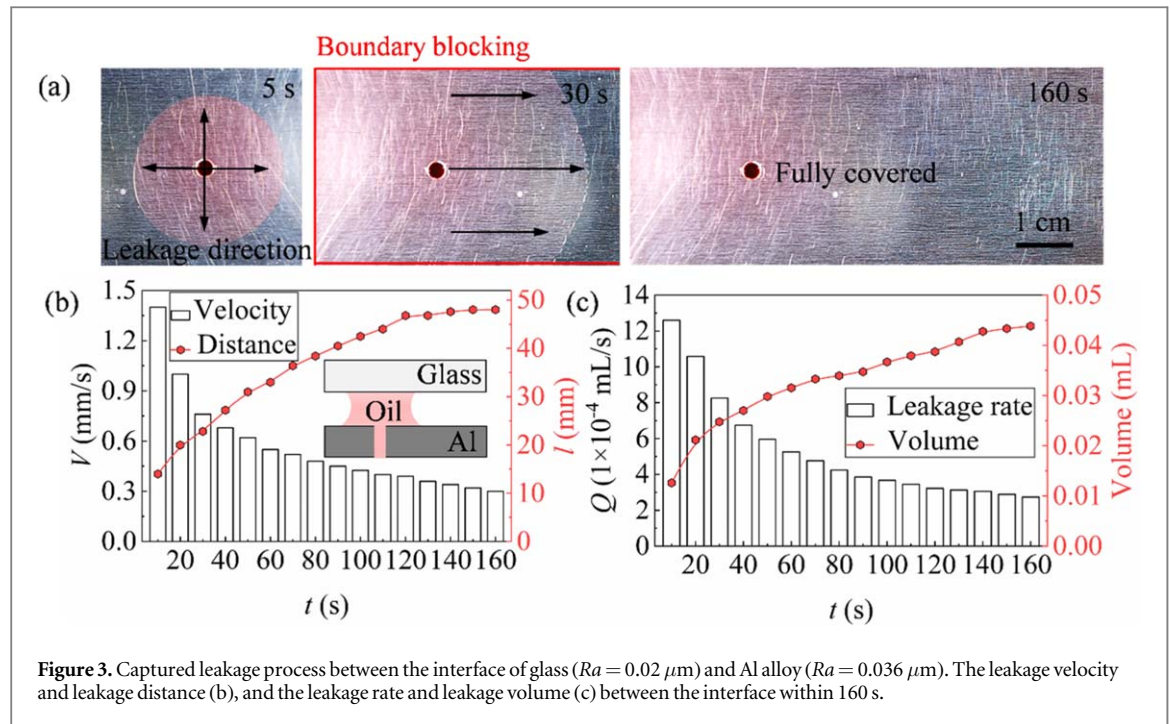
surfaces, which were measured by an optical interferometer microscopy (Contour GT, Bruker, USA) in the VSI model (an objective with a magnification of 2.5). R_a represented the roughness of the specimen surfaces and PSD represented the sample surface periodicity. Surface roughness (R_a) and Power spectral density (PSD) were obtained by its software (Vision 5.6), of which R_a represents the arithmetic mean deviation based on the line profile method, and PSD represents the degree of surface inhomogeneity at the corresponding spatial frequency [20], respectively. The detailed parameters are shown in table 2 and figure S1. From figure S1, untreated surface and irregular grinding scars surface exhibit inhomogeneity, and the rest of the surface shows periodicity. Referring to figure 1, the parallel and perpendicular grinding scars are defined as the direction of the x and y coordinate axes, respectively.

3. Results and discussion

3.1. Basic leakage performance

Figure 3 shows the leakage performance between the interface of the glass and Al plate under a contact pressure of 0.01 MPa, the surface roughness of glass is 0.02 μm, and the surface roughness of Al is 0.036 μm. Detailed leakage process with elapsed time is shown in figure 3(a). Initially, the oil spreads uniformly from the center to the surroundings (5 s), and once the oil reaches the boundary, it is blocked there and starts to spread in the same direction (30 s). The oil would cover the whole interface eventually (160 s). Figures 3(b) and (c) show the change trends of leakage velocity and leakage distance, and the leakage rate and leakage volume within a testing time of 160 s. It can be seen that with elapsed time, the distance increases, while the leakage velocity decreases gradually. Similarly, the leakage volume increases, while the leakage rate decreases as the leakage progresses.

Figure 4 presents the leakage behavior between the interface of glass ($R_a = 0.597 \mu\text{m}$) and Al alloy



($R_a = 0.654 \mu\text{m}$) under a contact pressure of 0.01 MPa. The orientation of the grinding scars of these two surfaces is parallel. Figures 4(a) and (b) show the change trends of leakage velocity and leakage distance, and the leakage rate and leakage volume within a testing time of 160 s. It can be seen that as the leakage progresses, the distance increases and the leakage velocity decreases gradually, while the leakage volume increases and the leakage rate decreases. Compared to the results in figure 3 the leakage rate is reduced when the contact surfaces have oriented grinding scars under the same experimental conditions.

3.2. Orientation effect on leakage performance

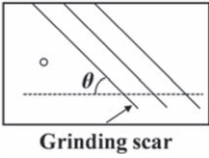
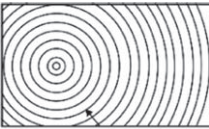
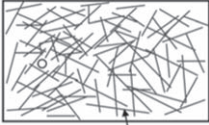
Figure 5 shows the leakage results between the interface of the smooth glass ($R_a = 0.02 \mu\text{m}$) and Al surfaces with different orientations of grinding scars ($R_a = \sim 0.6 \mu\text{m}$), and eight different interfaces are tested and compared. It can be seen from figure 5(a) that the orientation of grinding scars affects the leakage performance. For eight different interfaces, oil spreads from the center to the surrounding. For surfaces with circle, and surfaces with irregular grinding scars, the spread rate on these interfaces is all slower than those with oriented grinding scars. For surfaces with parallel, 30° , 45° , 60° , and perpendicular grinding scars, the leakage behavior for the surface with parallel grinding scars is most significant. the leakage velocity is fast. Figure 5(b) shows the maximum leakage distances (L_{max}) and minimum leakage distances (L_{min}) between different interfaces at 5 s. As shown in figure 5(b), for surfaces with oriented grinding scars, the difference between L_{max} and L_{min} is large, the difference for the surface with parallel grinding scars is most significant. For the surfaces with circle and irregular grinding

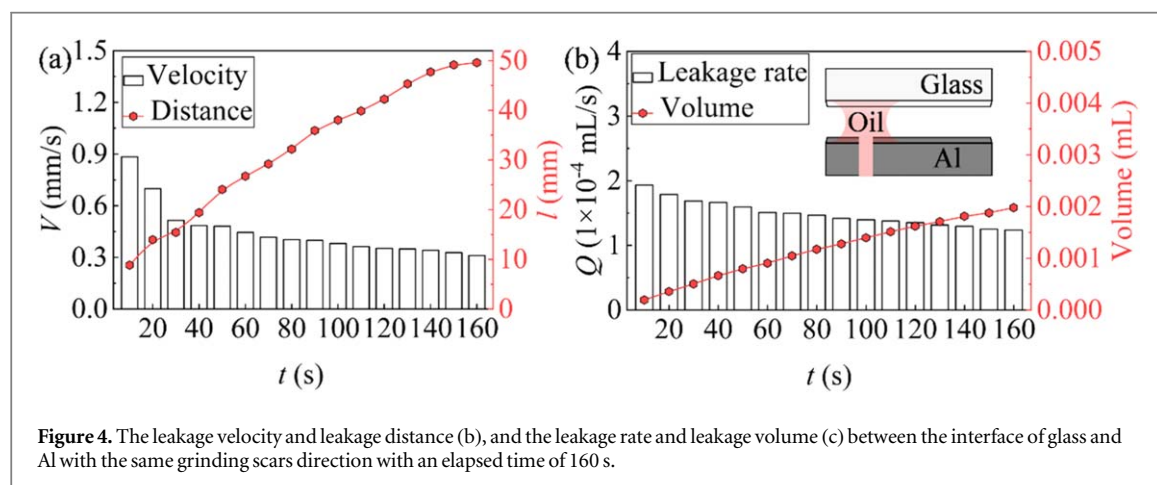
scars, the difference between L_{max} and L_{min} is small, and the oil flow at their interfaces shows isotropy.

Figure 5(c) presents the detailed results of the leakage rate under different contact pressures. Generally, the leakage rate decreases with increasing contact pressure. Note that surfaces with circle and irregular grinding scars have the best anti-leakage capability. Compared to the smooth one, they have a leakage suppression rate of approximately 85.9% and 84.4% under a contact pressure of 0.01 MPa. When the pressure increased to 0.07 MPa, the leakage suppression rate was approximately 85.6% and 84%, respectively. It is confirmed that the orientation of the grinding scars affects the leakage behavior, the leakage of the surface with parallel grinding scars is highest under different contact pressures, and the general leakage rate for these eight tested interfaces is in decreasing order of parallel, smooth, 30° , 45° , 60° , perpendicular, circle and irregular.

Figure 6 shows the leakage results between the interface of the glass and Al surfaces with different orientations of grinding scars ($R_a = \sim 0.6 \mu\text{m}$), and seven different interfaces are compared. Similar to the results in figure 5, the orientation of the grinding scars has a strong influence on the leakage performance. For surfaces with the orientation of grinding scars, it would leak along the grinding scars. For surfaces with circle and irregular grinding scars, the oil spreads uniformly from the center to the surrounding, and the velocity of spreading is slower than that for surfaces with the orientation of grinding scars. Figure 6(b) shows the maximum leakage distances (L_{max}) and minimum leakage distances (L_{min}) between different interfaces at 5 s. From figure 6(b), for surfaces with oriented grinding scars, the difference between L_{max}

Table 2. Parameters of all prepared surfaces.

Sketch map	Orientation of grinding scars (θ°)	Surface roughness ($Ra/\mu\text{m}$)	
		Al	Glass
 Grinding scar	Untreated	0.036	0.02
	Parallel	0.654, 2.033, 3.927	0.614, 2.097, 3.886
	30	0.619, 2.029, 3.976	0.622, 2.054, 3.922
	45	0.582, 1.996, 3.968	0.633, 1.979, 3.863
	60	0.677, 2.092, 4.036	0.617, 2.013, 3.924
 Grinding scar	Perpendicular	0.568, 1.987, 4.033	0.608, 2.109, 3.907
	Circle	0.695, 2.056, 4.027	0.61, 2.134, 3.869
 Grinding scar	Irregular	0.528, 2.096, 3.963	0.608, 2.107, 3.921



and L_{\min} is large, and the oil flow at these interfaces shows anisotropy. For the surfaces with circle and irregular grinding scars, the difference between L_{\max} and L_{\min} is small, and the oil flow at these interfaces shows isotropy.

Figure 6(c) shows the detailed results of the leakage rate under different contact pressures. It can be seen that the orientation of the grinding scars affects the leakage behavior, under the different contact pressure, the surface with parallel grinding scars has the highest leakage rate and velocity. As the orientation of the grinding scars shifts sequentially from parallel to

perpendicular, the leakage rate and leakage velocity gradually decrease. In addition, compared to the surfaces with oriented grinding scars, the surfaces with circle and irregular grinding scars show the best anti-leakage capability. Compared to the parallel abraded surfaces, they have a leakage suppression rate of approximately 70.2% and 68.9% under a contact pressure of 0.01 MPa. When the pressure was increased to 0.07 MPa, the leakage suppression rate was approximately 73.1% and 74.5%, respectively. Besides, the contact pressure affects the leakage behavior. When

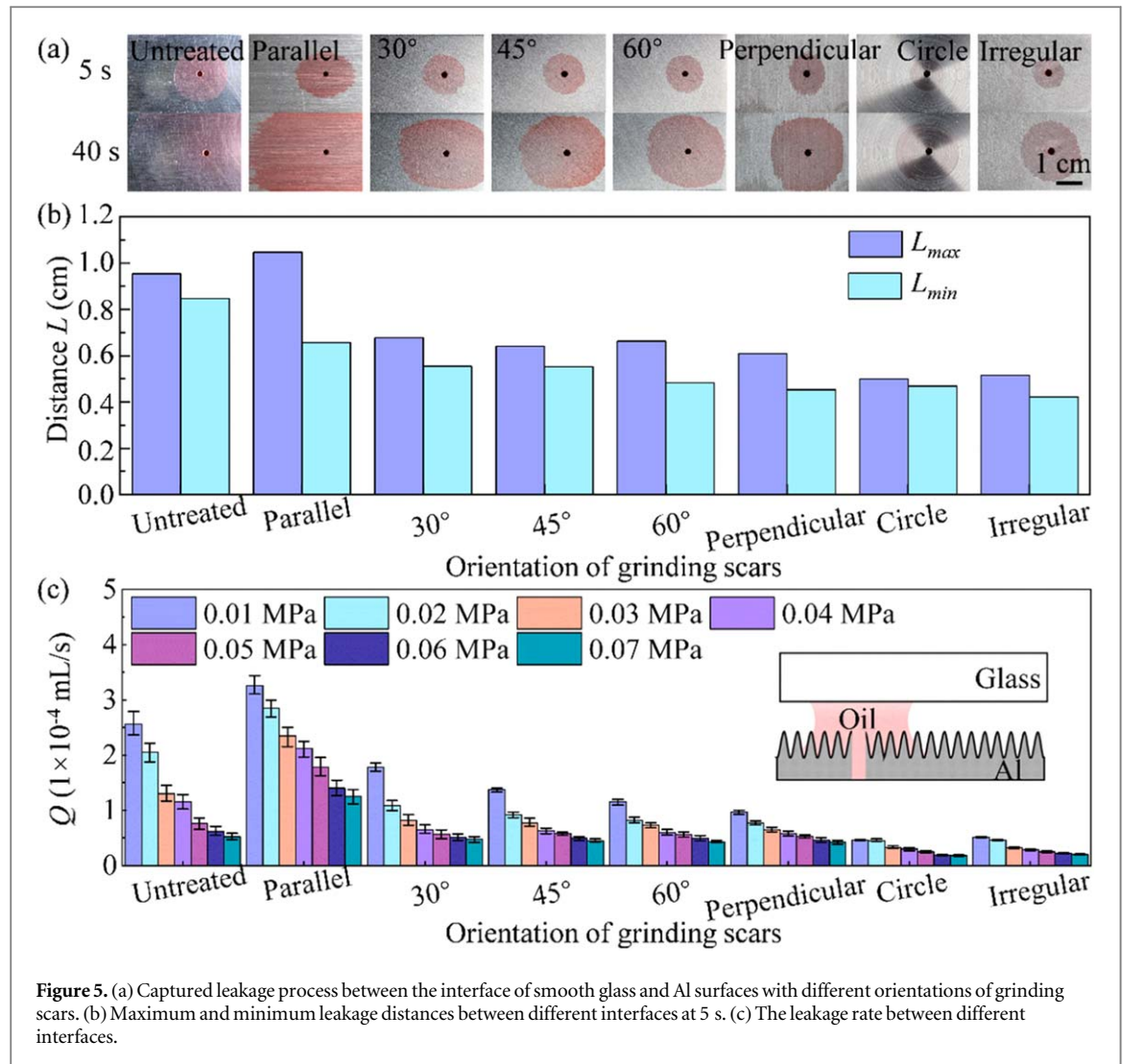


Figure 5. (a) Captured leakage process between the interface of smooth glass and Al surfaces with different orientations of grinding scars. (b) Maximum and minimum leakage distances between different interfaces at 5 s. (c) The leakage rate between different interfaces.

the contact pressure increases, its anti-leakage capability improves.

Compared to the results in figure 5, under the same experimental conditions, when both contact surfaces have grinding scars, the leakage rate is lower than that of a single surface with grinding scars.

3.3. Effect of roughness on leakage

Figure 7(a) presents the detailed results of the leakage rate between the interfaces of smooth glass and Al surfaces with different surface roughness ($R_a = \sim 4 \mu\text{m}$, $\sim 2 \mu\text{m}$, $\sim 0.6 \mu\text{m}$) under a contact pressure of 0.01 MPa. It can be found that surface roughness has a significant effect on leakage performance. For all tested interfaces, the leakage rate decreases with decreasing surface roughness. For surfaces with the circle and the irregular grinding scars, as the surface roughness decreases from 4 to $0.6 \mu\text{m}$, the leakage rates decreased by 74.9% and 72.3%, respectively.

Figure 7(b) shows the detailed results of leakage rate and leakage velocity between the interfaces of glass and Al surfaces with different surface roughness at a contact pressure of 0.01 MPa. Similar to the results in figure 7(a). It is seen that the surface roughness also

has a significant effect on the leakage performance. The surface roughness decreases for surfaces with different orientations of the grinding scars, while the leakage rate also decreases. For surfaces with the circle and the irregular grinding scars, as the surface roughness decreases from 4 to $0.6 \mu\text{m}$, the leakage rates decreased by 63.6% and 66.8%, respectively.

Comparing the results of figures 7(a) and (b), it is seen that the leakage rate of a single rough surface is higher than that of double rough surfaces.

Figures 8(a) and (b) show the distribution of leakage rate at different interfaces with the oriented scars and surface roughness. It can be seen that the orientation of scars and surface roughness have a significant effect on the leakage. When the surface of the seal has scars parallel to the leakage direction and a large roughness, the leakage rate is high. When the surface of the seal has a scar perpendicular to the leakage direction and a small roughness, the leakage rate is very low. Therefore, for the selection of seals, it is necessary to avoid the selection of surfaces with large roughness and grinding scars that are conducive to leakage.

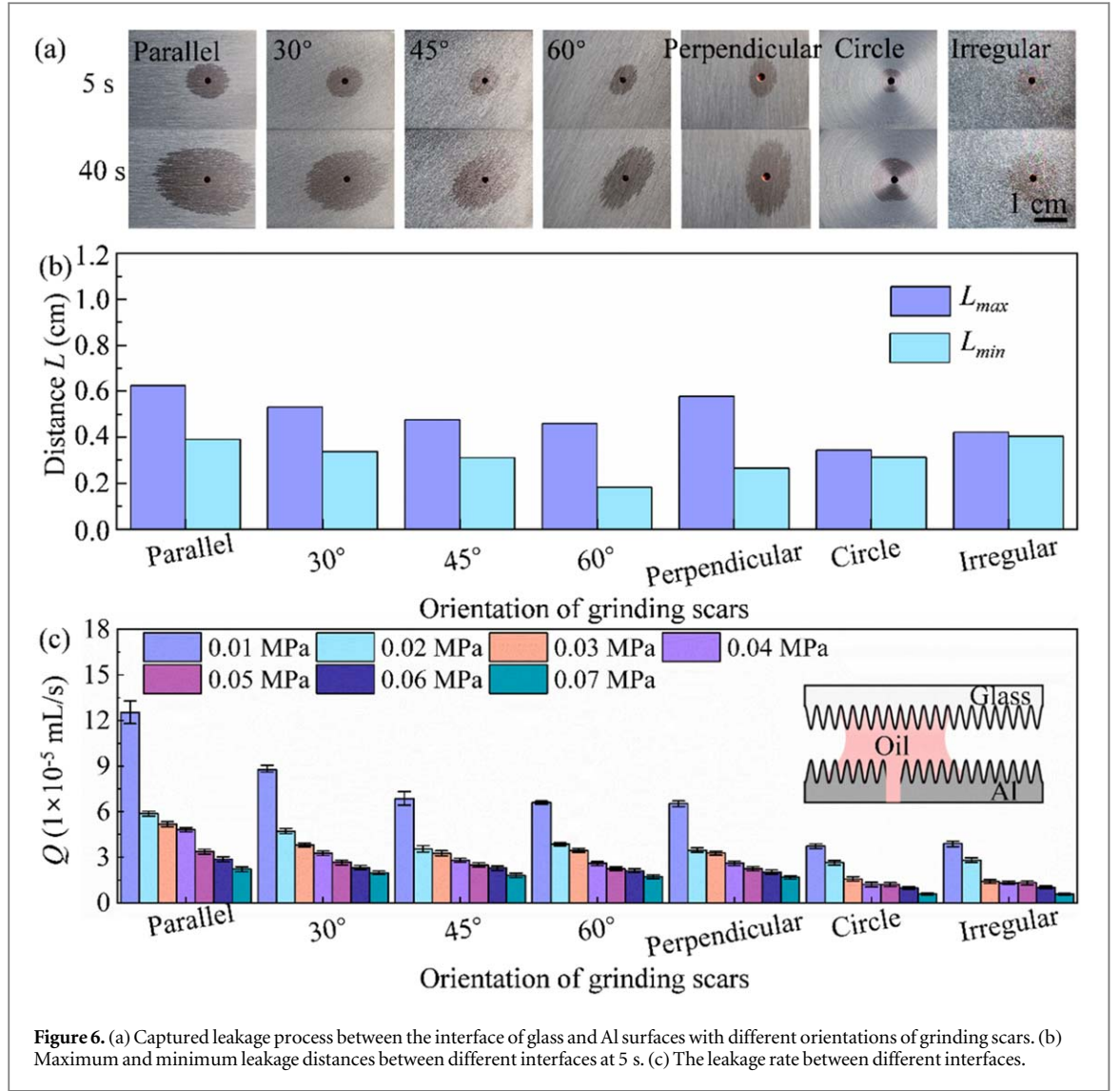


Figure 6. (a) Captured leakage process between the interface of glass and Al surfaces with different orientations of grinding scars. (b) Maximum and minimum leakage distances between different interfaces at 5 s. (c) The leakage rate between different interfaces.

3.4. Mechanism

To determine the leakage mechanism, the contact angle between different grinding scar surfaces in the x and y directions were measured (figure 9(a)). Contact angles on these testing surfaces were measured via a sessile droplet method, a 4 μ L drop deposited on a solid surface was taken within approximately 5 s after reaching the equilibrium state.

3.4.1. Surface grinding scars

It can be seen on the untreated surface, and surfaces with circle or irregular grinding scars, contact angles are similar in the x and y directions. There is a significant difference in the contact angles in both directions for surfaces with orientated grinding scars. For a surface with the parallel grinding scar, the contact angle in the x direction is smaller than that in the y direction. For a surface with the perpendicular grinding scar, the contact angle in the y direction is smaller than that in the x direction. It is because for droplets on the surfaces with orientated the grinding scar (figure 9(b)), due to the existence of micro-channels between the grinding scars, the oil droplet

will be spread along the grinding scar by its gravity as well as by capillary force [21], whereas perpendicular to the direction of the grinding scar, due to the influence of the boundary pinning effect [22, 23], the spreading of the oil is blocked by the grinding scar, which therefore results in the difference of the contact angle in different direction ($\theta_{//} < \theta_{\perp}$). It is well known that the pressure inside the droplet is related to the curvature of the liquid and the liquid-gas interfacial tension, which can be expressed by the Young-Laplace equation [24]:

$$\frac{dP}{dx} = -\frac{\gamma}{R^2} \frac{dR}{dx} \quad (3)$$

where P is the internal pressure of the droplet, R is the radius of curvature of the droplet interface, and γ is the liquid-gas interfacial tension of the droplet. As shown in figure 9(b), due to the $\theta_{//} < \theta_{\perp}$, the radius of curvature of the droplet in the parallel direction is larger than that of the droplet in the perpendicular direction ($R_{//} > R_{\perp}$). As indicated by equation (3), the internal pressure in the direction of parallel grinding scars is larger than that in the direction of

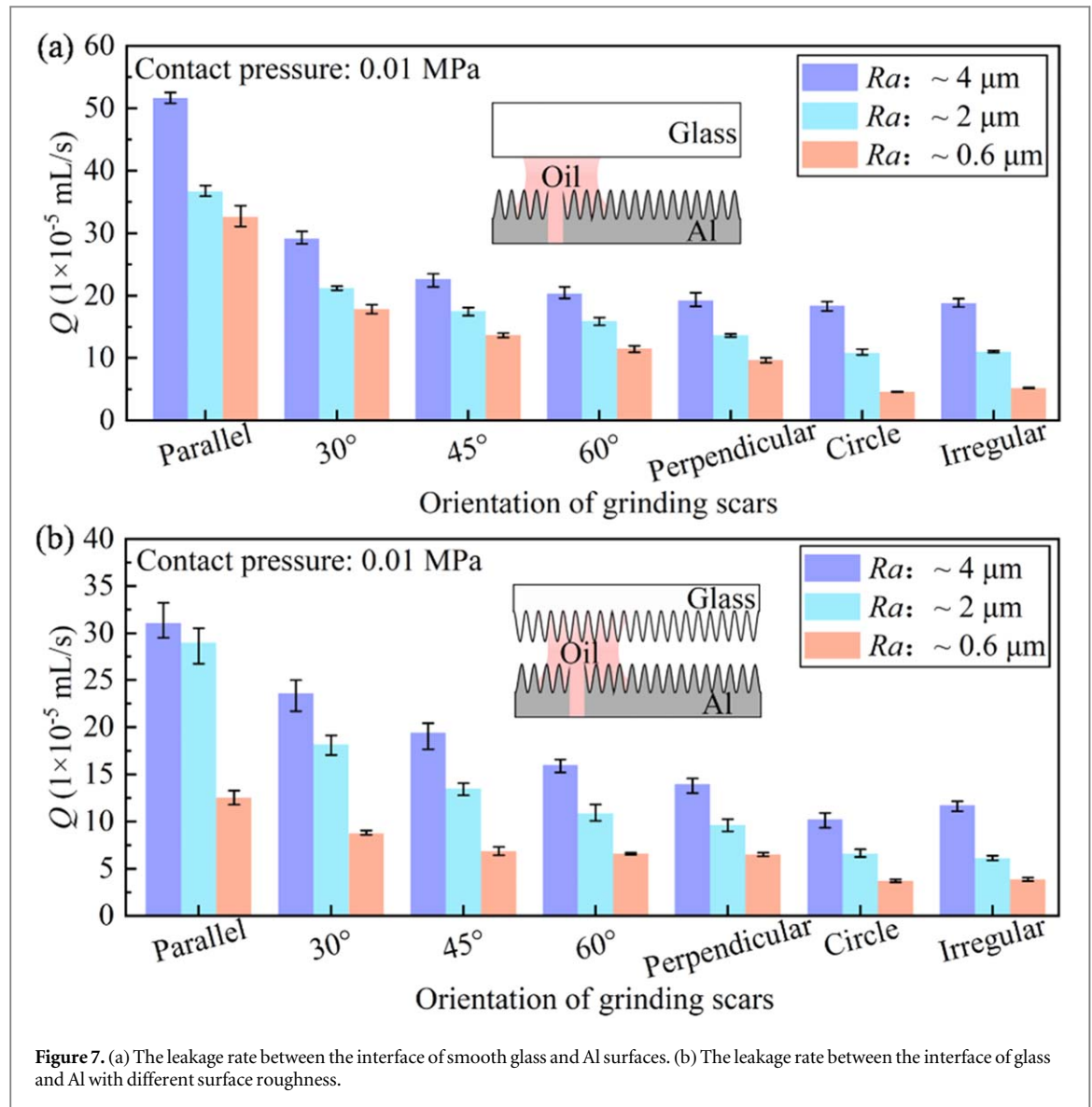


Figure 7. (a) The leakage rate between the interface of smooth glass and Al surfaces. (b) The leakage rate between the interface of glass and Al with different surface roughness.

perpendicular ($P_{//} > P_{\perp}$). That is, it is easier for the droplet to move along the direction of the grinding scars.

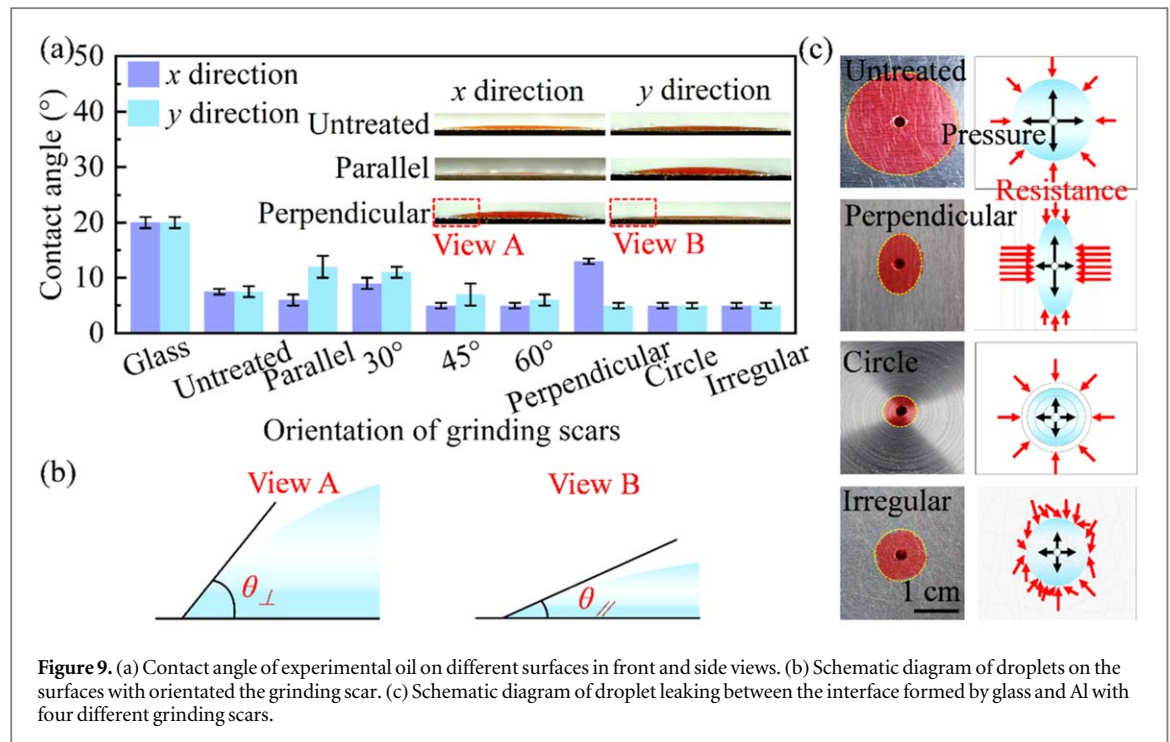
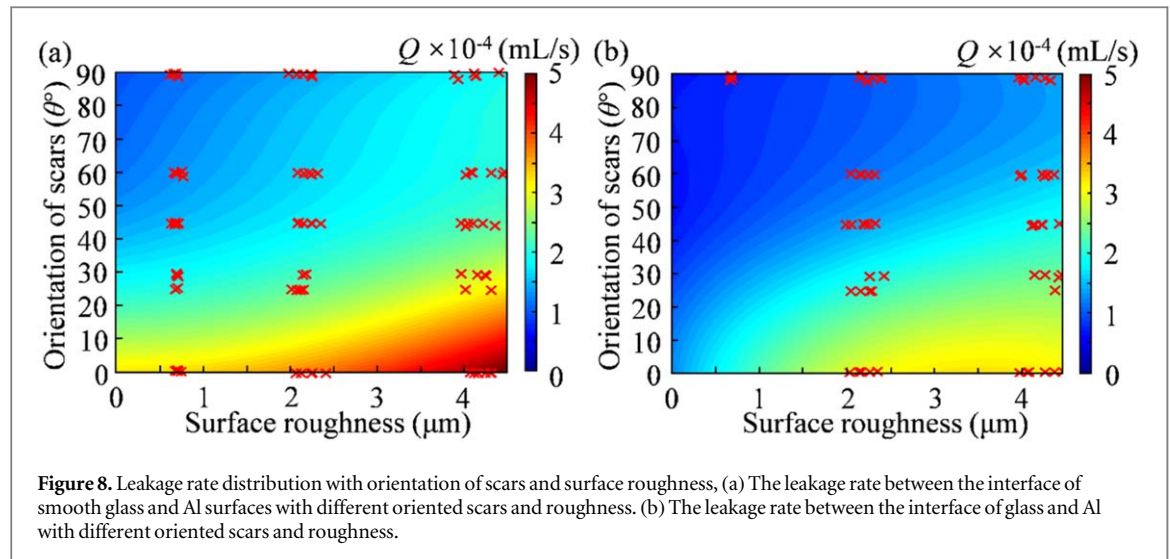
Figure 9(c) shows images and schematic diagrams of oil leaked between the interfaces of the untreated, perpendicular, circle, and irregular grinding scars. When the oil leaks at the interface formed by the untreated surface, the oil spreads uniformly from the center to the surroundings and is only subject to the frictional resistance f between the oil and the surface due to the smooth surface and the block of grinding scars. When the oil leakage direction is perpendicular to the direction of a single grinding scar, the oil will leak along the direction parallel to the grinding scar, and due to the blocking effect of the grinding scar, not only the frictional resistance f , but also the resistance of the grinding scar, would obstruct the leakage. When oil leaks between the interfaces formed by circle grinding scars, the leakage is blocked in omni-direction. Its anti-leakage capability is better than that of the perpendicular grinding scar surfaces. Since irregular grinding scar surfaces are not uniformly resisted by

scars compared to circle grinding scars due to a large number of irregularly, discontinuous grinding scars, it has a similar block effect.

Overall, the fabrication of suitable grinding scars on the specimen surfaces can delay leakage.

3.4.2. Difference between single and double-sided grinding scars

Since no machining method can produce an ideal smooth surface when two surfaces are extruded together, contact does not occur at every point, and micro-convexities at the contact interface extrude against each other, thus constituting actual contact [25]. For interfaces formed by smooth surfaces and rough sealing surfaces with grinding scars, the surfaces form a gap when they come into contact with each other under extrusion. The sealing medium passes through this space, resulting in leakage. For interfaces formed by rough surfaces with grinding scars, the micro-convexities on the two surfaces squeeze and engage each other when they come into contact with



each other under compression. At the same contact pressure, the volume of the gap formed is smaller than the gap between the interface formed by the smooth and grinding scars surfaces. Therefore, the leakage rate of the interface formed by the surface with the grinding scars is lower than that of the interface formed by the smooth surface and the grinding scars surfaces. For all interfaces, when the contact pressure is increased, the volume of the gap formed decreases or even disappears. As a result, the leakage rate is reduced.

To further explain the differences in leakage rates at interfaces formed by different surfaces, the schematic diagrams were shown in figure 10. Figure 10 shows the schematic diagrams of the oil in the interface formed by smooth surfaces, smooth and grinding scars surfaces, and grinding scars surfaces,

respectively. For the interface formed by smooth and grinding scars surfaces, due to the glass surface has low roughness ($Ra = 0.02 \mu\text{m}$), it can be simplified as an ideal smooth surface, the oil is only subjected to friction between itself and the upper surfaces (f_t). For the Al surfaces with different grinding scars, the oil is not only subjected to the friction between itself and the lower surfaces (f_b), but also from the grinding scars surface resistance F_{re} . Therefore, the total force exerted on the oil can be expressed as:

$$F_l = P_{in}S - f_t - f_b - F_{re} \quad (4)$$

where P_{in} is the inner pressure of the oil, S is the cross-sectional area between the interfaces, and f_t and f_b are the friction between the oil and the surface, respectively.

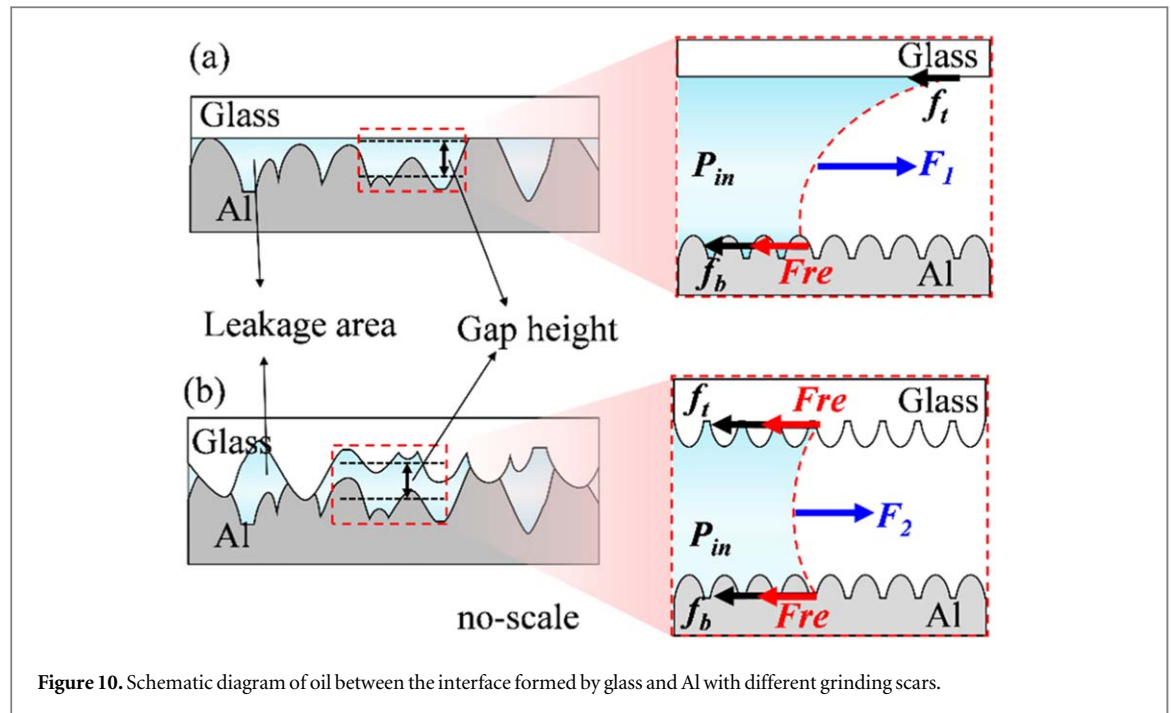


Figure 10. Schematic diagram of oil between the interface formed by glass and Al with different grinding scars.

For the interface formed by grinding scars surfaces, due to the grinding scars resistance on both surfaces, the total force can be written as:

$$F_2 = P_{in}S - f_t - f_b - 2F_{re} \quad (5)$$

Thus, compared with the interface formed by smooth surface and grinding scars surface, the leakage rate is further reduced.

3.4.3. Surface roughness

Surface roughness is the arithmetic mean of the absolute value of the profile offset over the sampling length. The size of the roughness determines the height of the gap that forms the interface (figure 10) [26]. As the roughness increases, the height and volume of the gap between the interfaces increase, and the number of leakage channels also increases [13], so the leakage rate increases. Therefore, leakage can be delayed by reducing the surface roughness of the sealing surfaces, selecting the appropriate direction of the grinding scars, and increasing the contact pressure.

4. Conclusions

In this study, the leakage behavior of contact static seals was investigated by a self-built experimental apparatus, and the effects of the surface topography (orientation of grinding scars) and roughness on the interface leakage under different contact pressures were studied. The following conclusions can be drawn from this work:

- (1) The leakage rate is negatively correlated with the contact pressure, the higher the contact pressure is, the slower the leakage will be.

- (2) The orientation of surface topography affects the leakage, for the grinding scar parallel to the leakage direction contributes to the leakage, and the perpendicular grinding scar has an inhibiting effect. The leakage rate of irregular and discontinuous surface topography is lower than that of regular ones.
- (3) The surface morphology plays a decisive role in the order of magnitude of the leakage rate, which means that the roughness is positively correlated with the leakage rate. That is, the rougher the surface, the greater the leakage rate.

Under the condition of meeting the machining process and structural requirements, the reduction of the leakage rate is achieved by reducing the surface roughness and by machining a block grinding scar. This work provides a general design guidance for the surface parameters optimization of static seals.

Acknowledgments

The authors are grateful for the financial support provided by the National Natural Science Foundation of China (Nos. 52175172 and 51805252).

Data availability statement

All data that support the findings of this study are included within the article (and any supplementary files).

Declarations

No potential conflict of interest was reported by the authors.

ORCID iDs

Qingwen Dai  <https://orcid.org/0000-0001-7422-4259>

Wei Huang  <https://orcid.org/0000-0002-8871-634X>

Xiaolei Wang  <https://orcid.org/0000-0002-9055-1011>

References

- [1] Wang R L, Liu J H, Zhang F K and Ding X Y 2021 An approach to evaluate the sealing performance of sealing structures based on multiscale contact analyses *Journal of Computational Design and Engineering* **8** 1433–45
- [2] Flitney R K 2011 *Seals and Sealing Handbook* (Elsevier)
- [3] Zhang Q, Chen X Q, Huang Y Y and Zhang X 2018 An experimental study of the leakage mechanism in static seals *Applied Sciences* **8** 1404
- [4] Zhang J and Hu Y 2019 Mechanical behavior and sealing performance of metal sealing system in roller cone bits *Journal Mechanical Science and Technology* **33** 2855–62
- [5] Liu T Q, Li X F, Liu S, Tian Y Q, Long J C, Xu C G and Sun K 2019 Analysis of Wedge-Shaped Contact Seal in Deep-Sea Sampler OCEANS-Marseille Conference (<https://doi.org/10.1109/oceanse.2019.8867547>)
- [6] Agarwal A 2014 An investigation on leakage behaviour of seals for aerospace applications *Master Thesis Delft University of Technology*
- [7] Arghavani J, Derenne M and Marchand L 2003 Effect of surface characteristics on compressive stress and leakage rate in gasketed flanged joints *International Journal of Advance Manufacturing Technology* **21** 713–32
- [8] Goltsberg R and Gilad M 2022 Experimental Study of the Sealing Performance of Metal on Polymer Conical Seals *J. Tribol.* **144** 062303
- [9] Marie C and Lasseux D 2007 Experimental leak-rate measurement through a static metal seal *J. Fluids Eng.* **129** 799–805
- [10] Hertz H 1881 On the contact of elastic solids *J. Reine Angew. Math* (Macmillan & Co) **92**, 156
- [11] Greenwood J A and Williamson J B P P 1996 Contact of nominally flat surfaces *Proc. R. Soc. A* **295** 300–19
- [12] Majumdar A and Bhushan B 1991 Fractal model of elastic-plastic contact between 17 rough surfaces *J. Tribol.* **113** 1–11
- [13] Sun J J, Ma C B, Lu J H and Yu Q P 2018 A leakage channel model for sealing interface of mechanical face seals based on percolation theory *Tribol. Int.* **118** 108–19
- [14] Sun J J, Ma C B, Yu Q P, Lu J H, Zhou M and Zhou P Y 2017 Numerical analysis on a new pump-out hydrodynamic mechanical seal *Tribol. Int.* **106** 62–70
- [15] Lorenz B and Persson B N J 2010 Leak rate of seals: effective-medium theory and comparison with experiment *Eur. Phys. J. E* **31** 159–67
- [16] Persson B N J and Yang C 2008 Theory of the leak-rate of seals *J. Phys. Condens. Matter* **20** 315011
- [17] Ni X Y, Sun J J, Zhang Y Y and Yu Q P 2021 A leakage model of contact mechanical seals based on the fractal theory of porous medium *Coatings* **11** 20
- [18] Yu R F and Chen W 2018 Fractal modeling of elastic-plastic contact between three-dimensional rough surfaces *Industrial Lubrication and Tribology* **70** 290–300
- [19] Zhang Q, Chen X Q, Huang Y Y and Chen Y 2018 Fractal modeling of fluidic leakage through metal sealing surfaces *AIP Adv.* **8** 045310
- [20] Liu Y H, Teng L, Li D Q and Zhang X 2006 Application of power spectral density to specify optical super-smooth surfaces *2nd International Symposium on Advanced Optical Manufacturing and Testing Technologies* **6** 15031
- [21] Chen S Q, Dai Q W, Yang X L, Liu J J, Huang W and Wang X L 2022 Bioinspired functional structures for lubricant control at surfaces and interfaces: wedged-groove with oriented capillary patterns *ACS Appl. Mater. Interfaces* **14** 42635–44
- [22] Yang X L, Zhuang K, Lu Y and Wang X L 2021 Creation of topological ultraslippery surfaces for droplet motion control *ACS Nano* **15** 2589–99
- [23] Dai Q W, Huang W, Wang X L and Khonsari M M 2021 Directional interfacial motion of liquids: fundamentals, evaluations, and manipulation strategies *Tribol. Int.* **154** 106749
- [24] Dai Q W, Huang W and Wang X L 2017 Micro-grooves design to modify the thermo-capillary migration of paraffin oil *Meccanica* **52** 171–81
- [25] Persson B N J, Albohr O, Creton C and Peveri V 2004 Contact area between a viscoelastic solid and a hard, randomly rough, substrate *J. Chem. Phys.* **120** 8779–93
- [26] Mayer E 1977 *Mechanical Seals 3rd*. (Newnes Butterworths)